University of Reading

Forecast error growth: a dynamic–stochastic model

Article

Published Version

Bach, E. ORCID: https://orcid.org/0000-0002-9725-0203, Crisan, D. and Ghil, M. (2025) Forecast error growth: a dynamic–stochastic model. Chaos: An Interdisciplinary Journal of Nonlinear Science, 35 (7). 073118. ISSN 1089-7682 doi: 10.1063/5.0248102 Available at https://centaur.reading.ac.uk/123533/

It is advisable to refer to the publisher's version if you intend to cite from the work. See Guidance on citing.

To link to this article DOI: http://dx.doi.org/10.1063/5.0248102

Publisher: American Institute of Physics

All outputs in CentAUR are protected by Intellectual Property Rights law, including copyright law. Copyright and IPR is retained by the creators or other copyright holders. Terms and conditions for use of this material are defined in the End User Agreement.

www.reading.ac.uk/centaur

CentAUR

University of Reading

Central Archive at the University of Reading

Reading's research outputs online

Chaos
An Interdisciplinary Journal of Nonlinear Science

RESEARCH ARTICLE | JULY 09 2025

Forecast error growth: A dynamic–stochastic model FREE

Eviatar Bach ; Dan Crisan ; Michael Ghil

Check for updates

Chaos 35, 073118 (2025)
https://doi.org/10.1063/5.0248102

View Online
Export Citation

09 July 2025 20:34:00

AIP Publishing
Chaos
Special Topics Open for Submissions
Learn More

AIP Publishing

Chaos ARTICLE pubs.aip.org/aip/cha

Forecast error growth: A dynamic–stochastic model

Cite as: Chaos 35, 073118 (2025); doi: 10.1063/5.0248102
Submitted: 10 November 2024 · Accepted: 25 June 2025 ·
Published Online: 9 July 2025

View Online Export Citation CrossMark

Eviatar Bach,[1,2,3,a)] Dan Crisan,[4,b)] and Michael Ghil[4,5,6,c)]

AFFILIATIONS

[1]Department of Environmental Science and Engineering and Department of Computing and Mathematical Sciences, California Institute of Technology, Pasadena, California 91125, USA
[2]Department of Meteorology and Department of Mathematics and Statistics, University of Reading, Reading RG6 6ET, United Kingdom
[3]National Centre for Earth Observation, Reading RG6 6ET, United Kingdom
[4]Department of Mathematics, Imperial College London, London SW7 2AZ, United Kingdom
[5]Geosciences Department and Laboratoire de Météorologie Dynamique (CNRS and IPSL), École Normale Supérieure and PSL University, Paris 75005, France
[6]Department of Atmospheric and Oceanic Sciences, University of California, Los Angeles, California 90095, USA

[a)]**Author to whom correspondence should be addressed:** eviatarbach@protonmail.com
[b)]**Electronic mail:** d.crisan@imperial.ac.uk
[c)]**Electronic mail:** ghil@lmd.ipsl.fr

ABSTRACT

There is a history of simple forecast error growth models designed to capture the key properties of error growth in operational numerical weather prediction (NWP) models. We propose here such a scalar model that relies on the previous ones and incorporates multiplicative noise in a nonlinear stochastic differential equation (SDE). We analyze the properties of this SDE, including the shape of the error growth curve for small times and its stationary distribution, and prove well-posedness and positivity of solutions. Next, we fit this model to operational NWP error growth curves and show good agreement with both the mean and probabilistic features of the error growth. These results suggest that the dynamic–stochastic error growth model proposed herein and similar ones could play a role in many other areas of the sciences that involve prediction.

Published under an exclusive license by AIP Publishing. https://doi.org/10.1063/5.0248102

09 July 2025 20:34:00

Quantifying and understanding forecast error growth plays a key role in prediction in many fields of the natural and socio-economic sciences. In addition to the extensive literature on the study of error growth in numerical weather prediction (NWP), this topic also plays an important role in understanding the limitations of prediction in other parts of the Earth system,[1] as well as in biology[2,3] and the social sciences.[4] Here, we propose a simple stochastic model to describe forecast error growth. We analyze its mathematical properties and show that it exhibits a good fit to real NWP error growth curves.

I. INTRODUCTION

Consider a dynamical system

$$\mathrm{d}x = f(x)\,\mathrm{d}t + \Sigma^{1/2}(x)\,\mathrm{d}B, \tag{1}$$

where Σ is a symmetric positive definite covariance matrix and B is a Wiener process. Given a true trajectory $x^\dagger(t)$ and a forecast trajectory $x(t)$, both generated by an equation like Eq. (1), one can measure the forecast error by

$$e^2(t) = \|x(t) - x^\dagger(t)\|_2^2, \tag{2}$$

where $\|\cdot\|_2$ is the Euclidean norm; other norms can also be considered. If $x^\dagger(0) \neq x(0)$ and the system is chaotic in the absence of noise, $e(t)$ will generally grow exponentially in time until reaching a saturation level (see Fig. 1 for a typical example). If the noise realization differs between $x^\dagger(t)$ and $x(t)$, the noise will also contribute to the error growth. Moreover, a model typically differs from the system being modeled—i.e., $x^\dagger(t)$ and $x(t)$ come from similar but not identical systems—and this systematic model error contributes to the error growth as well.

Published under an exclusive license by AIP Publishing

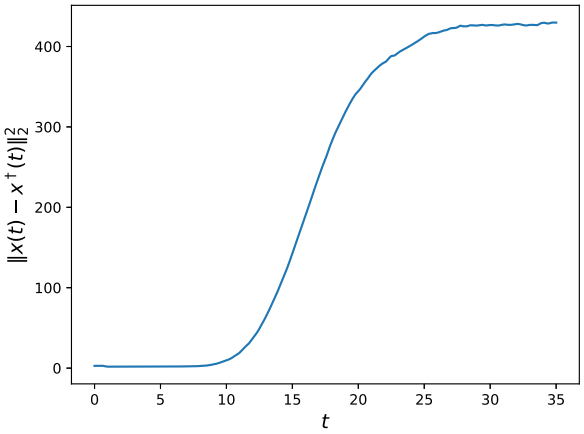

FIG. 1. A typical pattern of error growth for a chaotic dynamical system. The system used here is the chaotic convection model of Lorenz[5] with the parameter values $\rho = 28$, $\sigma = 10$, and $\beta = 8/3$. The error growth is averaged over many initial conditions and a moving average filter is applied.

A. Stochastic treatment of error growth

Suppose we have some uncertainty in the knowledge of the initial conditions $x^\dagger(0)$, represented by a probability distribution $\rho_0(x)$, such that $x^\dagger(0) \sim \rho_0(x)$. This probability distribution $\rho(x,t)$ will evolve under the dynamics according to the Fokker–Planck equation,

$$\frac{\partial \rho}{\partial t} = -\nabla \cdot (\rho f) + \frac{1}{2}\nabla \cdot (\nabla \cdot (\rho \Sigma)), \tag{3}$$

with $\rho(x,0) = \rho_0(x)$. In the above equation, the divergence of a matrix S, such as $\rho\Sigma$, is defined, for any vector a, by the identity $(\nabla \cdot S) \cdot a \equiv \nabla \cdot (S^T a)$, and $\nabla \cdot b$ is the divergence of a vector b.

If we further assume that a forecast was initialized from $x(0) \sim \rho_0$, then $x(t) \sim \rho(x,t)$, and $e(t)$ will be a random variable whose properties can be derived from those of $\rho(t)$. For example, the expected squared error satisfies

$$\mathbb{E}[e(t)^2] = \mathbb{E}\left[\|x(t) - x^\dagger(t)\|_2^2\right] \tag{4a}$$

$$= \mathbb{E}\left[\|x(t) - \mathbb{E}[x(t)]\|_2^2 + \|x^\dagger(t) - \mathbb{E}[x(t)]\|_2^2\right], \tag{4b}$$

$$= 2\mathrm{tr}(\mathrm{Cov}[x(t)]),$$

and the cross-covariance terms vanish because x and $x^\dagger$ are independent and identically distributed.

If $\rho(t)$ converges to a unique invariant measure, that is, $\rho(t) \to \rho_\infty$ as $t \to \infty$, then $\mathrm{Cov}[x(t)] \to C_\infty$, known in meteorological contexts as the climatological variance. When the forecast error reaches this climatological variance, the forecast has lost skill completely, and the forecast with the lowest error is the mean of ρ_∞, with an expected squared error of $\mathrm{tr}(C_\infty)$ (see Leith[6]). Additional statistical properties of $e(t)$ can also be studied.

In ensemble prediction, such as that used nowadays in NWP,[7] a set of M initial conditions drawn from ρ_0, $\{x^{(i)}\}_{i=1}^M$, are evolved in time under the dynamics equation (1). For a perfect ensemble, each ensemble member will be statistically indistinguishable from the true trajectory.[8] Thus, the error of each member will be a sample of the random variable $e(t)$ discussed above.

The preceding discussion shows that uncertainty in the initial conditions leads naturally to a probabilistic treatment of error growth, even in the case of a deterministic dynamical system where $\Sigma = 0$. Moreover, sources of error growth in deterministic systems that may nonetheless be modeled as stochastic include fluctuations in the finite-time Lyapunov exponents,[9] the impact of small and fast scales on large and slow ones, and model error.[10] Other works that took a probabilistic view on forecast error growth include Balgovind *et al.*,[11] Benzi and Carnevale,[12] Ehrendorfer,[10] Ivanov *et al.*,[13] and Chu and Ivanov.[14] Here, we do not deal with these sources of error explicitly, but do consider their cumulative effect.

B. Previous error growth models in NWP

Considerable attention has been given to forecast error growth in the forecast–assimilation (FA) cycle of operational NWP models, and a number of scalar error growth models have been proposed so far. For illustration purposes, we start by considering here four different models for error growth in NWP, namely, those of Leith,[15] Lorenz,[16] Dalcher and Kalnay,[17] and Nicolis[9] (see also Appendix A of Crisan and Ghil[18] and Krishnamurthy[19] for reviews of the literature).

Letting $v(t) = e(t)^2$, the forecast error model of Leith[15] is given by the scalar, linear inhomogeneous ordinary differential equation (ODE),

$$\frac{dv}{dt} = \alpha v + s, \tag{5}$$

where $\alpha > 0$ measures the rate of growth of small errors, s is the systematic model error, and t is the lead time. The solution to this ODE is given explicitly by

$$v(t) = \left(v_0 + \frac{s}{\alpha}\right) e^{\alpha t} - \frac{s}{\alpha}, \tag{6}$$

where $v_0 = v(0)$ is the initial error. Note that short-time forecast errors grow exponentially and that the systematic model error acts to increase the coefficient of this growth. Leith's forecast error model can only apply for short-time error growth, since it does not saturate.

Lorenz[16] proposed another model of forecast error growth that is governed by the following scalar ODE with quadratic right-hand side,

$$\frac{de}{dt} = ae(e_\infty - e), \tag{7}$$

where e_∞ is a saturation value. While Lorenz's model does include a nonlinear saturation term, it does not incorporate systematic model error.

The error model of Dalcher and Kalnay,[17] henceforth DK, combines the key features of the Leith and Lorenz models,

$$\frac{dv}{dt} = (\alpha v + s)(1 - v/v_\infty); \tag{8}$$

it thus, includes both a saturation level v_∞ and systematic model error s. For short-time error growth, we can take $v_\infty \to \infty$, recovering Leith's model. For $s = 0$, the model is similar to that of Lorenz. DK fit this error growth model to operational NWP forecasts from the European Centre for Medium-Range Weather Forecasting

09 July 2025 20:34:00

Published under an exclusive license by AIP Publishing

(ECMWF), finding close agreement out to 10 days. Zhang *et al.*[20] use the same model, up to a rescaling of variables, to estimate the predictability limit of midlatitude weather. Note that in previous works, s has been taken to represent sources of error other than systematic model error.[17,20]

Nicolis[9] proposed a stochastic error model of the form

$$\mathrm{d}\xi = (\sigma - g\xi)\xi\,\mathrm{d}t + q\xi\,\mathrm{d}W, \tag{9}$$

where ξ is a measure of error along the unstable direction, W is a Wiener process, and $g \geq 0$ and q are constants. To the best of our knowledge, this work is the only stochastic model of error growth previously proposed. Formulation (9) is justified in the paper by considering a toy model of the atmosphere and introducing stochasticity coming from fluctuations in the finite-time Lyapunov exponents. This model was also analyzed by Chu *et al.*[21] If we remove the stochasticity by setting $q = 0$, (9) has the same form as the Lorenz model. This model does not appear to have been calibrated to operational NWP error growth.

Other error growth models include those of Schubert and Suarez,[22] Stroe and Royer,[23] and Reynolds *et al.*[24]

In the present paper, we build on the previous error growth models above by adding multiplicative noise, as in the Nicolis model, to the DK model.

This paper is structured as follows. In Sec. II, we introduce the proposed stochastic model with multiplicative noise and study its properties, including its stationary distribution and first passage times. We then fit the model to operational NWP error curves in Sec. III. In Sec. IV, we discuss the results thus obtained. We also comment on the likelihood of these results applying to other areas of the sciences where prediction is important. In Appendix A, we prove well-posedness and positivity of our nonlinear stochastic model, with other model properties discussed in Appendixes B and C.

II. A STOCHASTIC ERROR GROWTH MODEL

A. Stochastic model formulation

We introduce multiplicative noise into the DK[17] model by writing the Itô stochastic differential equation (SDE),

$$\mathrm{d}v = (\alpha v + s)(1 - v/v_\infty)\,\mathrm{d}t + \sigma v\,\mathrm{d}W, \tag{10}$$

with W being a standard Wiener process and σ a constant. With $\sigma = 0$, this model reduces to the DK model. Figure 2 shows some sample realizations from this SDE for a particular choice of parameter values.

This error model differs from the Nicolis model in Eq. (9) as the latter has no equivalent to the term involving s. Note that v_∞ no longer corresponds exactly to the saturation value, as it did in the deterministic case. In Sec. II C, we consider two different definitions of a saturation value in the stochastic context: one is the maximizer of the stationary distribution, and the other is its expectation.

We chose multiplicative noise rather than additive noise since the former provided a better fit to operational NWP error curves (see Sec. III here and the heuristic justifications for multiplicative noise in Nicolis[9]). We will see in Appendix A that multiplicative noise leads, almost surely, to positive solutions given positive initial conditions. This property matters because the forecast error cannot be negative. A noise term that is a nonlinear function of v could also be tried.

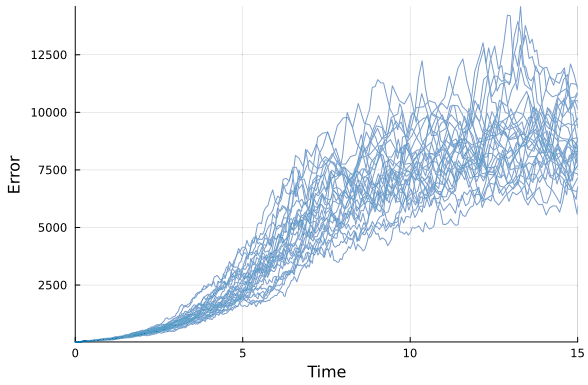

FIG. 2. Sample realizations of the SDE (10). Here, $v(0) = 30$ and the parameters are picked to be $v_\infty = 9000$, $\alpha = 0.6$, $s = 80$, and $\sigma = 0.2$.

For $s = 0$ and as $v/v_\infty \to 0$, the drift term becomes linear in v and the process becomes a geometric Brownian motion with solution

$$v(t) = v(0)\exp\left(\left(\alpha - \frac{\sigma^2}{2}\right)t + \sigma W\right), \tag{11}$$

with mean $\mathbb{E}[v(t)] = v(0)\exp(\alpha t)$ and variance $\mathrm{Var}[v(t)] = v(0)^2 \exp(2\alpha t)\left(\exp(\sigma^2 t) - 1\right)$. This formula approximately describes the small-time behavior of the process when $v(0) \ll v_\infty$, assuming that s is small.

Our model (10) also resembles that of stochastic logistic growth (see Liu and Wang[25]).

B. Nondimensionalization

Setting

$$T = \alpha^{-1}, \quad V = s\alpha^{-1}, \quad t^* = t/T, \tag{12a}$$

$$v^* = v/V, \quad v^*_\infty = v_\infty/V, \quad \beta = \sigma\alpha^{-1/2}, \tag{12b}$$

we obtain the nondimensional equation

$$\mathrm{d}v^* = (v^* + 1)\left(1 - \frac{v^*}{v^*_\infty}\right)\mathrm{d}t^* + \beta v^*\mathrm{d}W^*. \tag{13}$$

Thus, we have two nondimensional parameters, β and v^*_∞. The β parameter here is directly related to the λ parameter used by Chu *et al.*[21] for the Nicolis model. Note that this nondimensionalization can only be applied when $s \neq 0$. When $s = 0$, we will work with the dimensional equation (10).

In Appendix A, we show that if $v^*(0) > 0$, Eq. (13) has, almost surely, a unique and positive global solution.

09 July 2025 20:34:00

Published under an exclusive license by AIP Publishing

C. Fokker–Planck equation and stationary distribution

The Fokker–Planck equation that corresponds to Eq. (13) is

$$\frac{\partial \rho}{\partial t^*} = -\frac{\partial}{\partial v^*}\left[(v^*+1)\left(1-\frac{v^*}{v^*_\infty}\right)\rho\right] + \frac{\partial^2}{\partial v^{*2}}\left[\frac{\beta^2 v^{*2}}{2}\rho\right]. \quad (14)$$

We would like to find a stationary distribution ρ_∞ for which $\partial\rho_\infty/\partial t^* = 0$.

The detailed computations are provided in Appendix B. The resulting stationary distribution is

$$\rho_\infty(v^*) = D\,\exp\left(-\frac{2\left(\left(\beta^2 v^*_\infty - v^*_\infty + 1\right)\log(v^*) + \frac{v^*_\infty}{v^*} + v^*\right)}{\beta^2 v^*_\infty}\right); \quad (15)$$

here,

$$D = \frac{v^{*\,\frac{v^{*\,-1}_\infty - 1}{\beta^2} + \frac{1}{2}}_\infty}{2K_m\left(\frac{4}{v^{*\,1/2}_\infty \beta^2}\right)}, \quad m = \frac{2v^{*\,-1}_\infty - 2}{\beta^2} + 1, \quad (16)$$

and $K_n(z)$ is the modified Bessel function of the second kind, which satisfies $-y\left(n^2+z^2\right) + z^2 y'' + zy' = 0$.

Remark 1. Note that if $s = 0$, Eq. (15) reduces to Eq. (23) in Nicolis;[9] i.e., in dimensional variables,

$$\rho_\infty(v) = \frac{2^{\frac{2\alpha}{\sigma^2}-1} v^{\frac{2\alpha}{\sigma^2}-2}\left(\frac{\alpha}{\sigma^2 v_\infty}\right)^{\frac{2\alpha}{\sigma^2}-1} e^{-\frac{2\alpha v}{\sigma^2 v_\infty}}}{\Gamma\left(\frac{2\alpha}{\sigma^2}-1\right)}, \quad (17)$$

with $\alpha > \sigma^2/2$.

We find, furthermore, that ρ_∞ is unimodal, and maximized at

$$v^* = \frac{1}{2}\left(-\beta^2 v^*_\infty + \left[\left(\beta^2 v^*_\infty - v^*_\infty + 1\right)^2 + 4v^*_\infty\right]^{1/2} + v^*_\infty - 1\right). \quad (18)$$

As $t \to \infty$, $\mathbb{E}[v^*(t)]$ saturates. When related to the dynamical error growth, this saturation value should correspond to twice the climatological variance (see Sec. I A).

The limit of the expectation is

$$\lim_{t\to\infty} \mathbb{E}[v^*(t)] = \left(v^*_\infty\right)^{1/2} \frac{K_{m-1}\left(\frac{4}{v^{*\,1/2}_\infty \beta^2}\right)}{K_m\left(\frac{4}{v^{*\,1/2}_\infty \beta^2}\right)}, \quad (19)$$

and the limit of the variance is

$$\lim_{t\to\infty} \mathrm{Var}[v^*(t)] = \frac{v^*_\infty K_{-m+2}\left(\frac{4}{v^{*\,1/2}_\infty \beta^2}\right)}{K_m\left(\frac{4}{v^{*\,1/2}_\infty \beta^2}\right)} - \frac{v^*_\infty K_{m-1}\left(\frac{4}{v^{*\,1/2}_\infty \beta^2}\right)^2}{K_m\left(\frac{4}{v^{*\,1/2}_\infty \beta^2}\right)^2}. \quad (20)$$

D. First passage times and forecast skill horizons

A forecast is typically said to have lost skill when its error exceeds a certain threshold, e.g., some fraction of the climatological variance (see the discussion in Sec. I A). We can estimate the probability density function (PDF) of the times at which forecasts exceed a certain threshold v_c. These times have been previously referred to as first passage times.[13,21] When the threshold is used to measure the loss of prediction skill, then these first passage times have also been referred to as forecast skill horizons.[27]

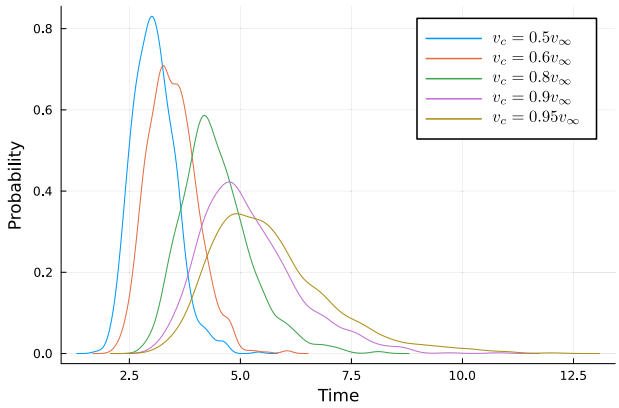

FIG. 3. Empirical PDFs of first passage times for solutions of the SDE, for increasing threshold values, from $v_c = 0.5v_\infty$ to $v_c = 0.95v_\infty$. Time in nondimensional units. The PDFs are estimated from data using kernel density estimation;[26] this is a likely reason for the small apparent deviations from unimodality.

Figure 3 shows empirical PDFs of first passage times for solutions of Eq. (10) with a given choice of parameters. We can see that these distributions tend to be positively skewed, i.e., the tail is toward larger first passage times. Moreover, the PDF flattens for higher values of the threshold.

Chu and Ivanov[14] examined in detail the distribution of first passage times for the Nicolis model of Eq. (9), including expressions for the moments of this distribution under various asymptotic regimes.

To summarize the skill horizon in a single number in this probabilistic perspective, we can consider:

(i) The skill horizon of an average forecast, $\min\{t : \mathbb{E}[v(t)] > v_c\}$.
(ii) The average skill horizon of a forecast, $\mathbb{E}[\min\{t : v(t) > v_c\}]$.

It may also be of interest to examine the tails of the first passage time PDFs, i.e., the probability of forecasts remaining skillful for an unusually long or short lead time.

E. Initial curvature

In Appendix C, we examine the curvature of the expectation of the stochastic model at time 0; compare Figs. 2–9 for an example of initially convex and initially concave expectation, respectively. We find that the curvature of the expectation, for a given deterministic initial condition v_0, is given by

$$\lim_{t\to 0} \frac{\mathrm{d}^2\mathbb{E}[v]}{\mathrm{d}t^2} = \left(\alpha - \frac{s}{v_\infty} - 2\frac{\alpha}{v_\infty}v_0\right)(\alpha v_0 + s)(1 - v_0/v_\infty) - \frac{\alpha}{v_\infty}\sigma^2 v_0^2. \quad (21)$$

Thus, the curvature at time 0 may be either concave or convex, depending on the parameter values and the initial condition. When

09 July 2025 20:34:00

Published under an exclusive license by AIP Publishing

the curve is initially convex, it will still be asymptotically concave, implying that there is an inflection point.

Equation (21) also shows that noise acts to decrease the initial curvature. Furthermore, a large enough σ guarantees that the error growth curve is concave throughout.

We note, however, that for the parameter values obtained from fits to NWP error growth in Sec. III, the curvature is always positive and far from becoming negative even with nonzero σ.

III. ERROR GROWTH IN THE SDE MODEL AND IN NWP MODELS

To determine the usefulness of the stochastic model, we fit it to error growth curves from operational NWP.

A. Forecasts and reanalysis data

We used forecasts of 500 hPa geopotential heights from the TIGGE dataset of ensemble forecasts.[28] This is a common variable used in predictability studies;[12] it corresponds roughly to the mid-level of the atmosphere, since the surface is, on average, at 1000 hPa. Within this dataset, we use the global 50-member ensemble forecasts from the European Centre for Medium-Range Weather Forecasting (ECMWF), initialized daily at 00 UTC on January 1–31, 2007. In these forecasts, the physics (parameterization) tendencies are stochastically perturbed to capture the uncertainty due to model errors.[29] See Fig. 4 for an example of the geopotential height field from the ensemble.

For each initialization time, we have $\binom{50}{2} = 1225$ pairs of forecasts. For the identical twin experiments below, we compute the mean-squared difference between each pair as a function of lead time. Since the data are provided on a latitude–longitude grid, the mean is weighted by the area of each grid cell to account for variations in the distance corresponding to a degree of longitude. We aggregate over all the initialization dates, resulting in a total of 37 975 error curves.

We also compute the error of each ensemble member with respect to reanalysis, taken to be an estimate of the true atmospheric state. We used the ERA5 reanalysis dataset.[30]

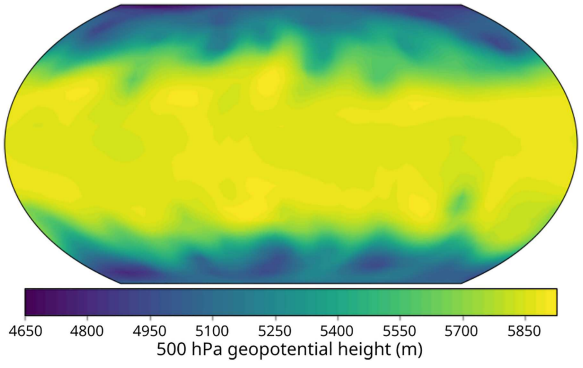

FIG. 4. Example of a geopotential height forecast ensemble member.

We compute the error of the forecasts, both for the identical twins and with respect to reanalysis, every 12 h for 10 days of lead time. Each error curve, thus, consists of 21 points.

B. Fitting procedure

We use ensemble Kalman inversion (EKI)[31] to fit the parameters of the SDE (10) to the NWP model error growth curves. EKI is derivative-free, which makes it an especially attractive method for parameter estimation in SDEs. It has previously been used for fitting SDE parameters in Schneider *et al.*[32] We only briefly describe EKI here (see also Chada,[33] Calvello *et al.*,[34] and Vernon *et al.*[35] for more detailed introductions).

EKI is an iterative ensemble method for approximately minimizing with respect to θ a cost function of the form

$$(y - \mathcal{G}(\theta))^\top \Gamma^{-1} (y - \mathcal{G}(\theta)). \tag{22}$$

Here, θ are the parameters one wishes to estimate, y are the observed data with noise covariance Γ, and $\mathcal{G}$ is the forward model that is assumed to have generated the data.

As the observations y, we take the logarithm of the mean and standard deviation of the error growth curves over time; since the error growth curve is 21 elements long (10 days sampled every 12 h), we obtain a vector with $n = 42$ components for each curve.

The logarithm of the data is taken in order to fit well both the initial and later portions of the error growth curve. We use the EnsembleKalmanProcesses.jl library,[36] with 100 ensemble members and 30 iterations, to calibrate v_∞, α, s, and σ parameters.

For all calibrations, except for the case of wavenumbers $k \geq 10$ described below, the initial ensembles were drawn from the distributions:

(a) v_∞ with mean 1.4×10^4 and standard deviation 5000, constrained to be positive;
(b) α with mean 0.6 and standard deviation 0.3, constrained to be positive;
(c) s with mean 200 with standard deviation 100, constrained to be positive; and
(d) σ with mean 0.2 and standard deviation 0.1, constrained to be between 0 and 1.

The means were chosen by rough inspection of solutions, while the standard deviations were chosen to be wide enough to explore a range of solutions. The constraints are implemented by calibrating in a transformed space and applying the inverse transformation to obtain the parameter estimates:[36] for the parameters constrained to be positive, we take the logarithm, and for the parameters constrained to be between 0 and 1, we apply the transformation $f(x) = \log(x/(1-x))$. Γ is set to be $0.25 I_n$. For the $k \geq 10$ case, due to the smaller magnitudes of the errors, we set Γ to be 40 times smaller, and the initial ensembles for v_∞ and s to have means and standard deviations 40 times smaller. The rest of the initial ensembles are left the same.

EKI begins with an initial ensemble of parameter sets and generates another ensemble of parameter sets at each iteration. For each parameter set, we generate 300 realizations of the SDE using the SRIW1 integrator in the DifferentialEquations.jl package[37] and compute the aforementioned statistics.

09 July 2025 20:34:00

Published under an exclusive license by AIP Publishing

In order to capture the initial spread of forecasts, each realization is initialized with a value of initial mean-square difference from a pair of forecasts in the identical twin case, and with a mean-square difference from the ensemble mean in the reanalysis case. EKI proceeds to update the ensemble of parameter sets using y and obtain the ensemble for the next iteration, converging toward parameter values that decrease the cost function (22).

C. Identical twins

We first look at the error growth as measured by the divergence of identical twins, i.e., of two ensemble members initialized at the same time. This approach is used to measure the error growth due to chaotic evolution of the system, and it is often used in the literature.[17] Note, however, that the error of individual ensemble members will be significantly larger than that of the ensemble mean, which is often used as the forecast. The impact of model error is partially captured in these forecasts by the stochastic perturbations to the physics tendencies.

Figure 5 shows the fit of the error growth model to the curves obtained by NWP. The mean as well as the plume of individual trajectories exhibits a good fit, except for a slight underestimation at later times. The fitted SDE model appears to begin to saturate around day 9, while the NWP does not; this could be remedied by using lead times beyond 10 days in the fitting procedure. The parameters are given in the first row of Table I; we also give the parameters for the fit for forecasts from the same system but initialized from July 1–31, 2007 in the fourth row.

In comparison to our results, Dalcher and Kalnay[17] found $v_\infty = 11\,076\,\mathrm{m}^2$, $\alpha = 0.43\,\mathrm{d}^{-1}$, and $s = 439\,\mathrm{m}^2\,\mathrm{d}^{-1}$ for boreal winter and $v_\infty = 9856\,\mathrm{m}^2$, $\alpha = 0.44\,\mathrm{d}^{-1}$, and $s = 597\,\mathrm{m}^2\,\mathrm{d}^{-1}$ for boreal summer. As expected, v_∞ is smaller in our results, due to the improvements in forecasting. As in the Dalcher and Kalnay[17] results, v_∞ was slightly smaller for summer than winter, and α was almost identical between the two seasons. However, we find a slightly smaller s for summer than winter, while Dalcher and Kalnay[17] found the opposite.

TABLE I. Parameters of the SDE error growth model estimated using the EKI procedure described in Sec. III B.

	v_∞ (m^2)	α (d^{-1})	s ($\mathrm{m}^2\,\mathrm{d}^{-1}$)	σ ($\mathrm{d}^{-1/2}$)
Identical twins	8 758	0.6062	109.7	0.2116
Identical twins $k \leq 9$	8 305	0.6419	83.08	0.2236
Identical twins $k \geq 10$	197.6	0.7853	8.709	0.2050
Identical twins, July	8 253	0.616	97.41	0.2120
Error with respect to reanalysis	10 530	0.4962	129.9	0.1859

For the identical twins, the best fits being provided by $s \neq 0$ can be explained by the stochastic physics, which are meant to capture the impact of systematic error on the growth in uncertainty. However, the fact that even for identical twins without stochastic physics the best fits were provided by $s \neq 0$ in Dalcher and Kalnay[17] and Zhang *et al.*[20] suggests that s can lead to a more realistic shape of the error growth curve even in the absence of this error. The results of Zhang *et al.*[20] cannot be directly compared to our results, since they use wind energy rather than geopotential height and also focus on midlatitudes.

Figure 6 presents the time-evolving PDFs of trajectories, and the fitted model again matches closely the NWP error curves. At 3 days, however, the SDE model underestimates the error systematically; by 6 days, this is no longer the case.

Figure 7 displays histograms of first passage times computed for different thresholds for NWP as well as for the fitted SDE model. The histograms are closely matched. Both also flatten at higher thresholds and are positively skewed, as suggested in Sec. II D.

D. Scale analysis

We repeated the identical twin experiments, but filtering the fields into low ($k \leq 9$) and high ($k \geq 10$) wavenumbers to measure the impact of spatial scale on error growth. For each of the

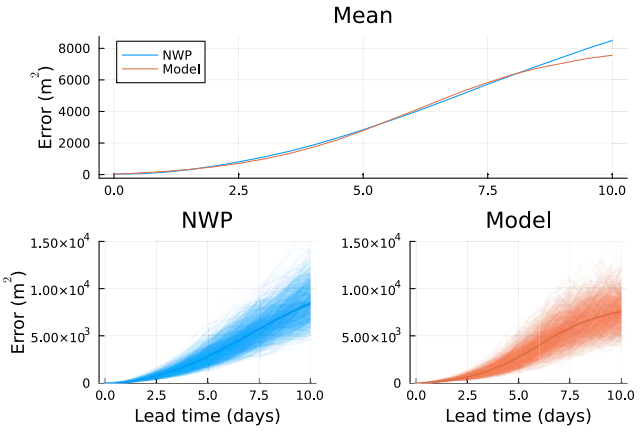

FIG. 5. Mean error growth curves. (a) For identical twins in an operational NWP forecast (blue curve) and the SDE model (red curve); (b) error growth of the individual NWP forecast pairs; and (c) realizations of the fitted SDE model.

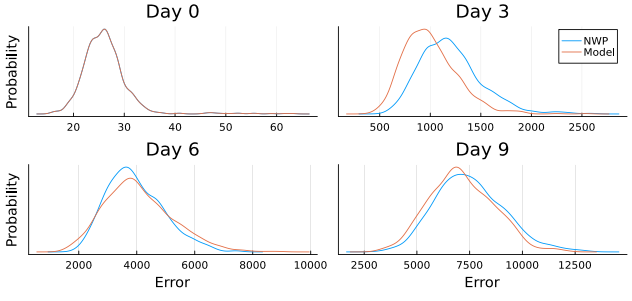

FIG. 6. PDFs of the error at increasing lead times for both the NWP data (blue curves) and the fitted SDE model (red curves). The PDFs are estimated from data using kernel density estimation.

09 July 2025 20:34:00

Published under an exclusive license by AIP Publishing

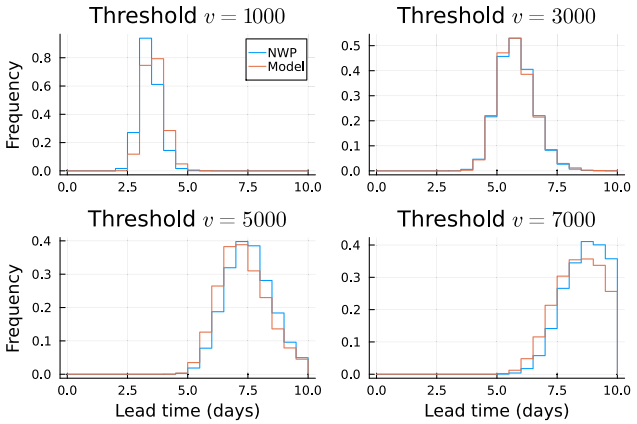

FIG. 7. Histograms of first passage times of NWP error growth and of the fitted SDE model at different threshold values. Error growth curves with a first passage time greater than 10 days were excluded.

wavenumber ranges, we filter the geopotential height fields and compute the mean-square error between the filtered fields.

The parameter values of the fits are summarized in Table I. The small scales exhibit a larger rate of error growth α, saturate more quickly, and have a similar degree of stochasticity in the error growth as the large scales. The model generally appears to fit the large-scale error growth better than the small scales (not shown).

E. Error with respect to reanalysis

We also compute the error curves of the NWP forecasts with respect to reanalysis, which includes the impact of systematic error. This is shown in Fig. 8, and the parameters are given in Table I. Again, the SDE model exhibits a good fit to NWP error growth.

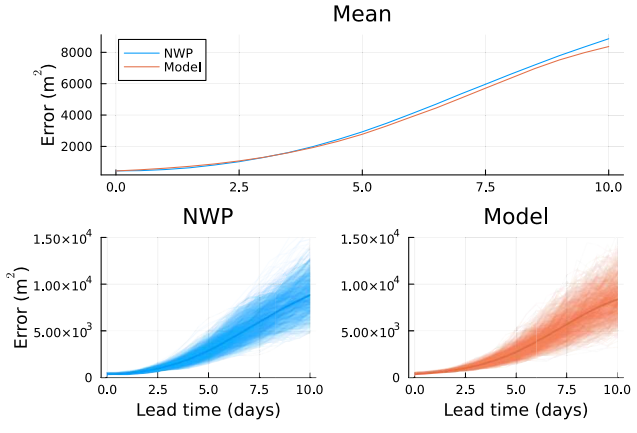

FIG. 8. Same as Fig. 5 but vs reanalysis. (a) For NWP forecasts with respect to reanalysis (blue curve) and the SDE model (red curve); (b) error growth of the individual NWP forecasts; and (c) realizations of the fitted SDE.

Because of the impact of systematic error, ν_∞ is considerably larger than that for the identical twin experiments. The best fit is provided by a smaller α but larger s than for identical twins. The larger s is expected since the systematic error is now directly contributing to the error growth.

IV. CONCLUDING REMARKS

We introduced a novel stochastic model of forecast error growth (10), building upon previous deterministic and stochastic models. Our nonlinear SDE model fits well the forecast error growth of the ECMWF's NWP model, accurately capturing both its mean and probabilistic aspects. Hence, the SDE model can be applied to quantify predictability in a probabilistic way.

Left for future work is the detailed analysis of the physical mechanisms leading to stochastic error growth, the application of this model to the forecast error growth of other systems, and its application to the analysis of predictability in the tropics compared to the extratropics.[38] While here we looked at the error growth of individual ensemble members in NWP, it may also be interesting to model the growth of probabilistic forecast skill scores, such as the continuous ranked probability score (CRPS).[39]

DEDICATION

This paper is dedicated to the memory of Eugenia Kalnay and to her fundamental contributions to research in predictability and weather forecasting.

ACKNOWLEDGMENTS

E. Bach was supported by the Foster and Coco Stanback Postdoctoral Fellowship at the California Institute of Technology. The work of D. Crisan has been partially supported by European Research Council (ERC) Synergy Grant (No. STUOD-DLV-856408). This is ClimTip contribution #45; the ClimTip project has received funding from the European Union's Horizon Europe research and innovation program under Grant Agreement No. 101137601. M. Ghil also received support from the French Agence Nationale de la Recherche (ANR) project TeMPlex under Grant Award No. ANR-23-CE56-1214 0002.

AUTHOR DECLARATIONS

Conflict of Interest

The authors have no conflicts to disclose.

Author Contributions

Eviatar Bach: Conceptualization (equal); Formal analysis (equal); Investigation (equal); Software (equal); Visualization (equal); Writing – original draft (equal); Writing – review & editing (equal). **Dan Crisan:** Conceptualization (equal); Formal analysis (equal); Investigation (equal); Writing – review & editing (equal). **Michael Ghil:** Conceptualization (lead); Formal analysis (supporting); Investigation (equal); Writing – review & editing (equal).

09 July 2025 20:34:00

Published under an exclusive license by AIP Publishing

DATA AVAILABILITY

Data sharing is not applicable to this article as no new data were created or analyzed in this study.

APPENDIX A: THE STOCHASTIC MODEL: POSITIVITY AND WELL-POSEDNESS

Theorem 1. *Equation (13) has a unique global solution* $\{v^*(t^*) : t^* \geq 0\}$, *P-almost surely for any initial value* $v^*(0) > 0$. *Moreover, the solution remains positive P-almost surely.*

Proof. First note that the coefficients of Eq. (13) are locally Lipschitz. It follows that, for any initial value $v^*(0) \in \mathbb{R}$, Eq. (13) has a unique maximal local strong solution on $[0, \tau)$, where τ is the explosion time (see, for example, Theorem 3.2.2, p. 95 in Mao[40]).

We show next that v^* cannot explode in finite time. More precisely, we show that P-almost surely $\tau = \infty$; in other words, Eq. (13) has a global solution, P-almost surely. To do this, we prove that v^* is bounded from above and from below by stochastic processes that are finite on the entire half line. Moreover, the lower bound process has sample paths of any solution that will never reach the origin, P-almost surely.

Lower bound. Observe that

$$(v^*+1)\left(1-\frac{v^*}{v^*_\infty}\right)+\chi(v^*)^2=\left(v^*\left(\frac{\frac{1}{v^*_\infty}-1}{2}\right)-1\right)^2,$$

where

$$\chi=\frac{\left(\frac{1}{v^*_\infty}-1\right)^2}{4}+\frac{1}{v^*_\infty}.$$

Hence,

$$(v^*+1)\left(1-\frac{v^*}{v^*_\infty}\right)\geq-\chi(v^*)^2.$$

By applying Proposition 2.18 in Karatzas and Shreve[41] we get that, P-almost surely, $v^* \geq v^*_{\text{low}}$, where v^*_{low} is the solution of the equation

$$\mathrm{d}v^*_{\text{low}}=-\chi\left(v^*_{\text{low}}\right)^2\mathrm{d}t^*+\beta v^*_{\text{low}}\,\mathrm{d}W^*. \tag{A1}$$

We emphasize that the inequality $v^* \geq v^*_{\text{low}}$ holds pathwise and not just in probability.

Equation (A1) has a unique maximal solution (again, say by Theorem 3.2.2, p. 95 in Mao[40]), that satisfies the identity

$$v^*_{\text{low}}(t^*)=v^*(0)\exp\left(\beta W_{t^*}-\frac{1}{2}\beta^2t^*-\int_0^{t^*}\chi\,v^*_{\text{low}}(s)\,\mathrm{d}s\right)>0.$$

In particular, v^*_{low} remains positive at all times and, therefore,

$$\begin{aligned}v^*_{\text{low}}(t^*)&=v^*(0)\exp\left(\beta W_{t^*}-\frac{1}{2}\beta^2t^*-\int_0^{t^*}\chi\,v^*_{\text{low}}(s)\,\mathrm{d}s\right)\\&<v^*(0)\exp\left(\beta W_{t^*}\right)\\&<\infty.\end{aligned}$$

It follows that Eq. (A1) has a unique *global* solution. Hence, v^* likewise stays positive on $[0, \tau)$ and, therefore, the explosion (if any) can only happen at $+\infty$. We show next that this is not possible either.

Upper bound. Observe that

$$(v^*+1)\left(1-\frac{v^*}{v^*_\infty}\right)+\gamma v^*-1=-\frac{1}{v^*_\infty}(v^*)^2,$$

where

$$\gamma=\frac{1}{v^*_\infty}-1.$$

Hence,

$$(v^*+1)\left(1-\frac{v^*}{v^*_\infty}\right)\leq-\gamma v^*+1.$$

Again, by applying Proposition 2.18 in Karatzas and Shreve[41] we get that, P-almost surely, $v^* \leq v^*_{\text{high}}$, where v^*_{high} is the solution of the equation

$$\mathrm{d}v^*_{\text{high}}=\left(-\gamma v^*_{\text{high}}+1\right)\mathrm{d}t^*+\beta v^*_{\text{high}}\,\mathrm{d}W^*. \tag{A2}$$

For linear or affine coefficients, Eq. (A2) has the unique global solution

$$v^*_{\text{high}}(t^*)=v^*(0)\exp\left(\beta W_{t^*}-\frac{1}{2}\beta^2t^*-\gamma t^*+t^*\right)<\infty.$$

In particular, it does not explode in finite time with probability 1, and, therefore, v^*, the solution of Eq. (13), will not explode at $+\infty$. The global existence of v^*, as well as its positivity, are now ensured. □

APPENDIX B: THE STOCHASTIC MODEL'S STATIONARY DISTRIBUTION

The Fokker–Planck equation that corresponds to Eq. (13) is

$$\frac{\partial\rho}{\partial t^*}=-\frac{\partial}{\partial v^*}\left[(v^*+1)\left(1-\frac{v^*}{v^*_\infty}\right)\rho\right]+\frac{\partial^2}{\partial v^{*2}}\left[\frac{\beta^2v^{*2}}{2}\rho\right].$$

We would like to find a stationary distribution ρ_∞, namely, solve $\partial\rho_\infty/\partial t^* = 0$.

We first take the integral with respect to v^*,

$$-(v^*+1)\left(1-\frac{v^*}{v^*_\infty}\right)\rho+\frac{\partial}{\partial v^*}\left[\frac{\beta^2v^{*2}}{2}\rho\right]=C, \tag{B1}$$

where C is an integration constant. The solution to Eq. (B1) is then

$$\rho_\infty(v^*)=A(v^*)\exp\left(-\frac{2\left(\left(\beta^2v^*_\infty-v^*_\infty+1\right)\log(v^*)+\frac{v^*_\infty}{v^*}+v^*\right)}{\beta^2v^*_\infty}\right),$$

where

$$A(v^*)=\int_1^{v^*}\frac{2C\exp\left(-\frac{2\left(\left(v^*_\infty-1\right)\log(V)-V-\frac{v^*_\infty}{V}\right)}{\beta^2v^*_\infty}\right)}{\beta^2}\mathrm{d}V+D, \tag{B2}$$

and D is another integration constant.

09 July 2025 20:34:00

Published under an exclusive license by AIP Publishing

Since the limit of the integrand in Eq. (B2) is infinite as $v^* \to \infty$ unless $C = 0$, a necessary condition for $\rho_\infty(v^*) \to 0$ as $v^* \to \infty$ is that $C = 0$. Then,

$$\rho_\infty(v^*) = D \exp\left(-\frac{2\left(\left(\beta^2 v_\infty^* - v_\infty^* + 1\right)\log(v^*) + \frac{v_\infty^*}{v^*} + v^*\right)}{\beta^2 v_\infty^*}\right).$$

The constant D can be eliminated using the normalization condition $\int_0^\infty \rho_\infty(v^*)\, dv^* = 1$,

$$D = \frac{{v_\infty^*}^{\frac{{v_\infty^*}^{-1}-1}{\beta^2}+\frac{1}{2}}}{2K_{\frac{2{v_\infty^*}^{-1}-2}{\beta^2}+1}\left(\frac{4}{{v_\infty^*}^{1/2}\beta^2}\right)},$$

where $K_n(z)$ is the modified Bessel function of the second kind, satisfying $-y\left(n^2+z^2\right)+z^2y''+zy'=0$.

APPENDIX C: INITIAL CURVATURE

Figure 9 shows sample realizations of the SDE where the expectation is concave at time 0; compare to Fig. 2 where the expectation is convex at time 0. We now determine the parameter values that lead the initial curvature to be either positive or negative.

Let us look at the deterministic DK model of Eq. (8),

$$\frac{dv^d}{dt} = (\alpha v^d + s)(1 - v^d/v_\infty),$$

where we assume that the initial condition $v_0 \le v_\infty$. Then,

$$\frac{d^2v^d}{dt^2} = \left(\alpha - \frac{s}{v_\infty} - 2\frac{\alpha}{v_\infty}v^d\right)\frac{dv^d}{dt}.$$

Note that asymptotically

$$\lim_{v^d \to v_\infty}\left(\alpha - \frac{s}{v_\infty} - 2\frac{\alpha}{v_\infty}v^d\right) = -\alpha - \frac{s}{v_\infty} < 0.$$

In other words, the function is concave in the asymptotic regime. We have two cases:

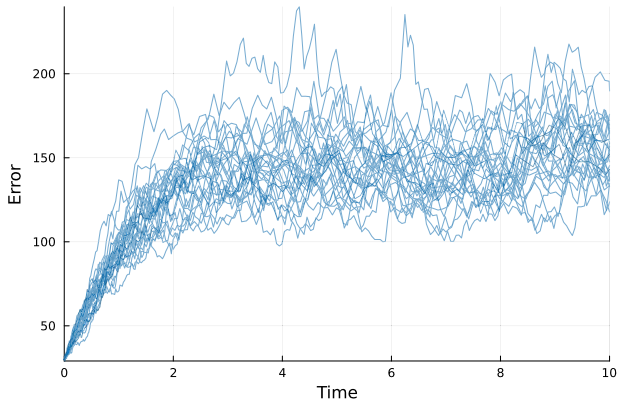

FIG. 9. Sample realizations of SDE (10) with concave expectation at time 0. Here, $v(0) = 30$ and parameters are $v_\infty = 150$, $\alpha = 0.6$, $s = 80$, and $\sigma = 0.2$.

- If $\alpha - \frac{s}{v_\infty} - 2\frac{\alpha}{v_\infty}v_0 \le 0$, then $\frac{d^2v^d}{dt^2} < 0$ on the interval $(0, \infty)$ and, therefore, the function is strictly concave on the interval $(0, \infty)$.
- If $\alpha - \frac{s}{v_\infty} - 2\frac{\alpha}{v_\infty}v_0 > 0$, then there exists t_c such that the function is convex on $(0, t_c)$ and concave on (t_c, ∞); in other words, t_c is an inflection point.

Returning to the stochastic model of Eq. (10), we find that

$$\frac{d\mathbb{E}[v]}{dt} = (\alpha\mathbb{E}[v] + s)(1 - \mathbb{E}[v]/v_\infty) - \frac{\alpha}{v_\infty}\mathrm{Var}[v]$$

and

$$\frac{d^2\mathbb{E}[v]}{dt^2} = \left(\alpha - \frac{s}{v_\infty} - 2\frac{\alpha}{v_\infty}\mathbb{E}[v]\right)\frac{d\mathbb{E}[v]}{dt} - \frac{\alpha}{v_\infty}\frac{d\mathrm{Var}[v]}{dt}.$$

We would like to get the limit at 0 of the derivative of the variance. Using Itô's lemma,

$$dv^2 = 2v(\alpha v + s)(1 - v/v_\infty)dt + 2\sigma v^2 dW + \sigma^2 v^2 dt,$$

$$\frac{d\mathbb{E}\left[v^2\right]}{dt} = 2\mathbb{E}\left[v(\alpha v + s)(1 - v/v_\infty)\right] + \sigma^2\mathbb{E}[v^2],$$

$$\frac{d\mathbb{E}[v]^2}{dt} = 2\mathbb{E}[v]\,(\alpha\mathbb{E}[v] + s)(1 - \mathbb{E}[v]/v_\infty) - 2\mathbb{E}[v]\,\frac{\alpha}{v_\infty}\mathrm{Var}[v].$$

If we assume a deterministic initial condition v_0, then

$$\lim_{t\to 0}\frac{d\mathbb{E}\left[v^2\right]}{dt} = 2v_0(\alpha v_0 + s)(1 - v_0/v_\infty) + \sigma^2 v_0^2,$$

$$\lim_{t\to 0}\frac{d\mathbb{E}[v]^2}{dt} = 2v_0(\alpha v_0 + s)(1 - v_0/v_\infty),$$

$$\lim_{t\to 0}\frac{d\mathrm{Var}[v]}{dt} = \sigma^2 v_0^2,$$

$$\lim_{t\to 0}\frac{d^2\mathbb{E}[v]}{dt^2} = \left(\alpha - \frac{s}{v_\infty} - 2\frac{\alpha}{v_\infty}v_0\right)(\alpha v_0 + s)(1 - v_0/v_\infty)$$

$$- \frac{\alpha}{v_\infty}\sigma^2 v_0^2 < \lim_{t\to 0}\frac{d^2v^d}{dt^2}.$$

Hence, $\lim_{t\to 0} d^2\mathbb{E}[v]/dt^2$ will be negative for sufficiently high σ^2; in other words, the expectation is a concave function in a neighborhood of 0.

REFERENCES

[1] A. Wirth and M. Ghil, "Error evolution in the dynamics of an ocean general circulation model," Dyn. Atmos. Oceans **32**, 419–431 (2000).
[2] M. E. Baird and I. M. Suthers, "Increasing model structural complexity inhibits the growth of initial condition errors," Ecol. Complexity **7**, 478–486 (2010).
[3] S. Pei and J. Shaman, "Counteracting structural errors in ensemble forecast of influenza outbreaks," Nat. Commun. **8**, 925 (2017).
[4] J. D. Farmer and F. Lafond, "How predictable is technological progress? Res. Policy **45**, 647–665 (2016).
[5] E. N. Lorenz, "Deterministic nonperiodic flow," J. Atmos. Sci. **20**, 130–141 (1963).
[6] C. E. Leith, "Theoretical skill of Monte Carlo forecasts," Mon. Weather Rev. **102**, 409–418 (1974).
[7] E. Kalnay, "Historical perspective: Earlier ensembles and forecasting forecast skill," Q. J. R. Meteorol. Soc. **145**, 25–34 (2019).

09 July 2025 20:34:00

Published under an exclusive license by AIP Publishing

[8]T. Palmer, R. Buizza, R. Hagedorn, A. Lawrence, M. Leutbecher, and L. Smith, "Ensemble prediction: A pedagogical perspective," ECMWF Newsl. **106**, 10–17 (2006).
[9]C. Nicolis, "Probabilistic aspects of error growth in atmospheric dynamics," Q. J. R. Meteorol. Soc. **118**, 553–568 (1992).
[10]M. Ehrendorfer, "The Liouville equation and its potential usefulness for the prediction of forecast skill. Part I: Theory," Mon. Weather Rev. **122**, 703–713 (1994).
[11]R. Balgovind, A. Dalcher, M. Ghil, and E. Kalnay, "A stochastic-dynamic model for the spatial structure of forecast error statistics," Mon. Weather Rev. **111**, 701–722 (1983).
[12]R. Benzi and G. F. Carnevale, "A possible measure of local predictability," J. Atmos. Sci. **46**, 3595–3598 (1989).
[13]L. M. Ivanov, J. Kirwan, and O. V. Melnichenko, "Prediction of the stochastic behaviour of nonlinear systems by deterministic models as a classical time-passage probabilistic problem," Nonlinear Process. Geophys. **1**, 224–233 (1994).
[14]P. C. Chu and L. M. Ivanov, "Linear and nonlinear perspectives of forecast error estimate using the first passage time," in *Symposium on Observations, Data Assimilation, and Probabilistic Prediction* (American Meteorological Society, Orlando, FL, 2002), pp. 127–132.
[15]C. E. Leith, "Objective methods for weather prediction," Annu. Rev. Fluid Mech. **10**, 107–128 (1978).
[16]E. N. Lorenz, "Atmospheric predictability experiments with a large numerical model," Tellus **34**, 505–513 (1982).
[17]A. Dalcher and E. Kalnay, "Error growth and predictability in operational ECMWF forecasts," Tellus A **39**, 474–491 (1987).
[18]D. Crisan and M. Ghil, "Asymptotic behavior of the forecast-assimilation process with unstable dynamics," Chaos **33**, 023139 (2023).
[19]V. Krishnamurthy, "Predictability of weather and climate," Earth Space Sci. **6**, 1043–1056 (2019).
[20]F. Zhang, Y. Q. Sun, L. Magnusson, R. Buizza, S.-J. Lin, J.-H. Chen, and K. Emanuel, "What is the predictability limit of midlatitude weather? J. Atmos. Sci. **76**, 1077–1091 (2019).
[21]P. C. Chu, L. M. Ivanov, T. M. Margolina, and O. V. Melnichenko, "Probabilistic stability of an atmospheric model to various amplitude perturbations," J. Atmos. Sci. **59**, 2860–2873 (2002).
[22]S. D. Schubert and M. Suarez, "Dynamical predictability in a simple general circulation model: Average error growth," J. Atmos. Sci. **46**, 353–370 (1989).
[23]R. Stroe and J. F. Royer, "Comparison of different error growth formulas and predictability estimation in numerical extended-range forecasts," Ann. Geophys. **11**, 296–316 (1993).
[24]C. A. Reynolds, P. J. Webster, and E. Kalnay, "Random error growth in NMC's global forecasts," Mon. Weather Rev. **122**, 1281–1305 (1994).
[25]M. Liu and K. Wang, "A note on stability of stochastic logistic equation," Appl. Math. Lett. **26**, 601–606 (2013).
[26]T. Hastie, R. Tibshirani, and J. Friedman, *The Elements of Statistical Learning*, 2nd ed., Springer Series in Statistics (Springer, New York, 2009).
[27]R. Buizza and M. Leutbecher, "The forecast skill horizon," Q. J. R. Meteorol. Soc. **141**, 3366–3382 (2015).
[28]P. Bougeault, Z. Toth, C. Bishop, B. Brown, D. Burridge, D. H. Chen, B. Ebert, M. Fuentes, T. M. Hamill, K. Mylne, J. Nicolau, T. Paccagnella, Y.-Y. Park, D. Parsons, B. Raoult, D. Schuster, P. S. Dias, R. Swinbank, Y. Takeuchi, W. Tennant, L. Wilson, and S. Worley, "The THORPEX interactive grand global ensemble," Bull. Am. Meteorol. Soc. **91**, 1059–1072 (2010).
[29]R. Buizza, M. Milleer, and T. N. Palmer, "Stochastic representation of model uncertainties in the ECMWF ensemble prediction system," Q. J. R. Meteorol. Soc. **125**, 2887–2908 (1999).
[30]H. Hersbach, B. Bell, P. Berrisford, S. Hirahara, A. Horányi, J. Muñoz-Sabater, J. Nicolas, C. Peubey, R. Radu, D. Schepers, A. Simmons, C. Soci, S. Abdalla, X. Abellan, G. Balsamo, P. Bechtold, G. Biavati, J. Bidlot, M. Bonavita, G. D. Chiara, P. Dahlgren, D. Dee, M. Diamantakis, R. Dragani, J. Flemming, R. Forbes, M. Fuentes, A. Geer, L. Haimberger, S. Healy, R. J. Hogan, E. Hólm, M. Janisková, S. Keeley, P. Laloyaux, P. Lopez, C. Lupu, G. Radnoti, P. de Rosnay, I. Rozum, F. Vamborg, S. Villaume, and J.-N. Thépaut, "The ERA5 global reanalysis," Q. J. R. Meteorol. Soc. **146**, 1999–2049 (2020).
[31]M. A. Iglesias, K. J. H. Law, and A. M. Stuart, "Ensemble Kalman methods for inverse problems," Inverse Probl. **29**, 045001 (2013).
[32]T. Schneider, A. M. Stuart, and J.-L. Wu, "Learning stochastic closures using ensemble Kalman inversion," Trans. Math. Appl. **5**, tnab003 (2021).
[33]N. K. Chada, "A review of the EnKF for parameter estimation," in *Inverse Problems—Recent Advances and Applications* (IntechOpen, 2022).
[34]E. Calvello, S. Reich, and A. M. Stuart, "Ensemble Kalman methods: A mean field perspective," arXiv:2209.11371[cs,math] (2024).
[35]S. Vernon, E. Bach, and O. R. A. Dunbar, "Nesterov acceleration for ensemble Kalman inversion and variants," J. Comp. Phys. **535**, 114063 (2025).
[36]O. R. A. Dunbar, I. Lopez-Gomez, A. Garbuno-Iñigo, D. Z. Huang, E. Bach, and J.-L. Wu, "EnsembleKalmanProcesses.jl: Derivative-free ensemble-based model calibration," J. Open Source Software **7**, 4869 (2022).
[37]C. Rackauckas and Q. Nie, "DifferentialEquations.jl—A performant and feature-rich ecosystem for solving differential equations in Julia," J. Open Res. Software **5**, 15 (2017).
[38]E. Bach, S. Motesharrei, E. Kalnay, and A. Ruiz-Barradas, "Local atmosphere-ocean predictability: Dynamical origins, lead times, and seasonality," J. Clim. **32**, 7507–7519 (2019).
[39]H. Hersbach, "Decomposition of the continuous ranked probability score for ensemble prediction systems," Weather Forecast. **15**, 559–570 (2000).
[40]X. Mao, *Stochastic Differential Equations and Applications* (Woodhead Publishing, 2007).
[41]I. Karatzas and S. E. Shreve, *Brownian Motion and Stochastic Calculus*, Graduate Texts in Mathematics Vol. 113 (Springer, New York, 1998).

09 July 2025 20:34:00

Published under an exclusive license by AIP Publishing